A&A 386, 854–859 (2002)
DOI: 10.1051/0004-6361:20020270

Astronomy & Astrophysics

Near infrared observations of soft X-ray selected AGN*

D. Grupe[1] and H.-C. Thomas[2]

[1] MPI für extraterrestrische Physik, Postfach 1312, 85741 Garching, Germany
[2] MPI für Astrophysik, Karl-Schwarzschild-Str. 1, 85748 Garching, Germany

Received 19 December 2001 / Accepted 20 February 2002

Abstract. We report the results of near infrared observations of 19 soft X-ray selected AGN. The goal of the observations was to search for strong, narrow Paα or Brγ emission lines, as a sign of nuclear starbursts. We found Paα emission in the spectra of 11 sources and Brγ in at least five. Strong NIR emission has been found in two sources, CBS 126 and Mkn 766, both objects with strong [OIII]λ5007 emission, weak Fe II emission and wavelength dependent degree of polarization in the optical. Classical Narrow Line Seyfert 1 galaxies do not show exceptionally strong NIR emission lines. We present the results of our study and discuss how our findings fit into an evolutionary scheme of AGN.

Key words. accretion, accretion disks – galaxies: active – galaxies: nuclei – galaxies: Seyfert

1. Introduction

Optical spectra of AGN exhibit many significant relationships. For example, increasing strength of Fe II emission from the broad line region (BLR) corresponds to decreasing width of Hβ from the BLR, and decreasing strength of [O III] λ5007 emission from the narrow line region (NLR) (Boroson & Green 1992; Grupe et al. 1999). ROSAT (Trümper 1983), with its high sensitivity to soft X-rays, has played an important role in showing that these trends correspond to an increasing steepness of the soft X-ray spectra (Boller et al. 1996; Wang et al. 1996; Laor et al. 1997; Grupe et al. 1998a). Correlation analyses show that the dominant spectrum-to-spectrum variation in AGN samples can be reduced to a linear combination of these emission line and continuum parameters – the "First Principal Component" (Boroson & Green 1992).

The "First Principal Component" (or Eigenvector 1) almost certainly represents the Eddington ratio $L/L_{\rm Edd}$, where L is the bolometric luminosity, and $L_{\rm Edd}$ is the upper limit to a Black Hole's luminosity for which radiation forces on the accreting matter balance gravitational forces (e.g., Boroson 2002). Narrow Line Seyfert 1 nuclei (NLS1), with their steeper X-ray spectra, stronger Fe II, weaker [O III] emission and narrower Hβ represent higher Eddington ratios, and are therefore suggested to be an earlier stage of activity (Grupe 1996; Grupe et al. 1999; Mathur 2000), or a rejuvenated phase of Seyfert 1 activity. The association between AGN activity and starbursts is well documented (e.g. Gonzáles Delgado 2001; Cid Fernandes et al. 2001 and references therein). Starbursts, perhaps triggered by galaxy mergers or interactions, are usually associated with fueling the central engine, although it has been suggested that AGN activity triggers the starbursts. The AGN-starburst connection has been demonstrated for Seyfert 2 galaxies where about 30–50% do show massive young stars within ~300 pc of the center (Cid Fernandes et al. 2001). Consistent with this, Wills et al. (1999) suggested that starbursts could provide the high-column densities of dense, Fe-enriched gas suggested by Principal Component 1 spectra. Starburst galaxies are known to be bright in the infrared. Therefore we would expect to see higher IR luminosities in NLS1 than in broad line Seyfert 1s (BLS1). We found that soft X-ray selected AGN on the average show slightly higher IR luminosities than AGN from hard X-ray selected samples (Grupe et al. 1998a; Moran et al. 1996). However, among the most luminous infrared objects, the ultra-luminous IRAS galaxies (ULIRGs), AGN appear to be rare (Murphy et al. 2001) and recently Ivanov et al. (2000) found from a K-band spectroscopy study of 33 Seyfert galaxies that there is no evidence for strong starbursts among their sources. At optical/NIR wavelengths one way to indicate a starburst in nearby bright galaxies is to measure the strength of the CaII triplett ($\lambda\lambda$8498, 8542, 8662 Å; e.g. Terlevich et al. 1990). However, while in the optical it is not (easily) possible to distinguish between the activity from the nucleus itself and a circumnuclear starburst, it

Send offprint requests to: D. Grupe,
e-mail: `dgrupe@xray.mpe.mpg.de`

* Based on observations performed at the 2.7 m telescope of the McDonald Observatory, Texas.

is (easier) in the infrared (e.g. Genzel & Cesarsky 2000; Laurent et al. 2000).

In principle, near infrared (NIR) spectroscopy provides a tool to distinguish between young and old starbursts by searching for strong hydrogen emission lines from young stars or CO absorption lines at 2.3 μm from old stars (Heisler & De Robertis 1999). These CO absorption lines have been found to be common in obcured AGN while they are absent in Seyfert 1s (Oliva et al. 1999).

We observed 19 sources of our complete sample of 113 soft X-ray selected AGN (Grupe et al. 2001) by NIR spectroscopy in the K-band. The sources were selected from the ROSAT All-Sky Survey (RASS, Voges et al. 1999) by their count rate and hardness ratio (Thomas et al. 1998; Grupe et al. 1998a). In this paper we present the results of a first observing run to study the soft X-ray selected AGN of our sample in the infrared. We have organized this paper as follows: in Sect. 2 we describe the observation and the data reduction and analysis, in Sect. 3 the results of our NIR study are presented, and are discussed in Sect. 4.

2. Observations and data reduction

The near-infrared spectroscopy of our AGN subsample used the CoolSpec spectrograph (Lester et al. 2000) on the 2.7 m telescope at McDonald Observatory in Texas. We used grating #3310-FL-906 in the K-band in first order with a resolution $\lambda/\Delta\lambda = 268$ and a 256×256 NICMOS3 CCD ($\Delta\lambda$ at 2.2 μm $\equiv$ 2.6 pixel). Table 1 lists all sources with the optical positions, redshifts, K magnitudes from the 2 Micron All Sky Survey (2MASS) second incremental release catalogue, observed K magnitude $K_{\rm obs}$, and observing dates and times. During the whole run the weather conditions were rather poor, therefore absolute flux calibrations are not very accurate. In order to obtain these we observed for each object a nearby bright star of spectral type A to G. The spectral types were taken from the Bright Source Catalogue, 5th revised edition (Hoffleit & Jaschek 1991). For some of our comparison stars the K magnitudes were known, for others the K magnitudes were derived from the B and V magnitudes using the relation $V-K = (2.29 \pm 0.01) \times (B-V)$. This relation was obtained by fitting the colours in a sample of 196 infrared standard stars common to the list of Van der Bliek et al. (1996) and the Bright Star Catalogue, 5th Revised Ed. (Hoffleit & Jaschek 1991). These K magnitudes were converted into flux densities at 2.2 μm using the relation $K = 14.0–2.5 \log(F_{2.2\mu})$ (Van der Bliek et al. 1996) with the flux density in units of 10^{-15} W m^{-2} μm^{-1}. The flux density distribution in our observing window was then computed from the flux density at 2.2 μm assuming a Rayleigh-Jeans tail for the spectral shape.

The flux-calibrated spectrum of the AGN can then be calculated from the ratio of the observed spectra of AGN and comparison star, taking into account the different exposure times. The flux densities at 2.2 μm thus obtained for our AGN were converted into K magnitudes using the relation given above. In Table 1 we list these K magnitudes together with those given in the 2MASS catalogue. In most cases the observed magnitude is less than the one given in the 2MASS, because the poor weather conditions are more likely to reduce the flux for the long exposures of the objects than for the short exposures of the comparison stars. In this way we can scale the observed AGN spectrum, to account for variations in the extinction between source and comparison star and we are able to get more reliable absolute infrared fluxes that can be compared to our measurements in the optical range. As listed in Table 1 for six sources K magnitudes were not yet available in the 2MASS. Therefore we give line fluxes in Table 2 only for those sources for which we could do the scaling as described above.

Wavelength calibrations were obtained by fitting a linear relation to the line positions of Argon, Neon, and Xenon. Sky subtraction was done by nodding the telescope between two positions in a star-sky-sky-star sequence. For our targets such a sequence took 8 min and was repeated several times, while for the bright comparison stars a much shorter exposure time of 4 to 20 s per sequence was sufficient.

3. Results

Figure 1 displays all NIR spectra of the 19 soft X-ray selected AGN we observed as well as a mean spectrum of the atmospheric absorption. Out of 12 sources with redshifts that put Paα into the observable window the Paα line was clearly detected in 11 cases. The much weaker Brγ line should have been visible for 11 sources. Of those sources it was clearly detected in Mkn 766 and possibly in RX J0859+48, Mkn 110, CBS 126, and IRAS 12397+3333. In the other 6 sources, where Brγ is marked in the spectrum, it is not clear if this is noise or a real line. Therefore in Table 2 the Brγ measurements of those sources are noted as upper limits. Upper limits were estimated from the noise peaks in the spectrum. Due to the redshift of the sources for only a few objects it is possible to get the Paα as well as the Brγ line.

Table 2 lists the results from the line measurements. The table contains the object name (as given in Table 1), the Seyfert type, the rest frame equivalent widths of Paα and Brγ and the rest frame $FWHM$(Paα). The $FWHM$(Paα) (in Å) was deconvolved by the spectral resolution of about 180 Å, using $FWHM(\mathrm{Pa}\alpha_{\rm corr})^2 = FWHM(\mathrm{Pa}\alpha_{\rm observed})^2 - 180^2$. The Pa$\alpha$ line widths are in agreement with other studies in the literature (e.g. Hines 1991). The table also contains the line fluxes of Paα and Brγ and the Paα/Hβ line ratio. The Hβ line flux was measured from FeII subtracted optical spectra (Grupe et al. 1999). The cases are marked in the table, for which absolute fluxes can not be given, because no 2MASS data are available yet.

Two of the sources listed in Table 2 show exceptionally high Paα/Hβ flux ratios, CBS 126 and RX J1355.2+5612. From the case B scenario (Hummer & Storey 1987) a

Table 1. List of the AGN; α_{2000} and δ_{2000} are the optical positions (Grupe et al. 2001), K magnitudes are taken from the 2MASS catalogue and from the observed spectrum (before scaling), and $T_{\rm obs}$ lists the total observing time per source in minutes.

#	Name	α_{2000}	δ_{2000}	z	$K_{\rm 2MASS}$	$K_{\rm obs}$	Obs date	$T_{\rm obs}$	comp. star	spec. type
1	RX J0859.0+4846	08 59 02.9	+48 46 09	0.083	—	12.3	2001-02-18	24	HR 2692	G9V
2	Mkn 110	09 25 13.0	+52 17 12	0.035	—	12.5	2001-02-18	32	HR 4096	A2V
3	PG0953+414	09 56 52.4	+41 15 22	0.234	12.5	12.4	2001-02-19	16	HR 3811	F2V
4	RX J1005.7+4332	10 05 41.9	+43 32 41	0.178	12.7	12.9	2001-02-17	32	HR 4067	F7V
5	RX J1007.1+2203	10 07 10.2	+22 03 02	0.083	14.2	14.0	2001-02-19	32	HR 4012	F9V
6	CBS 126	10 13 03.2	+35 51 24	0.079	12.6	13.0	2001-02-18	24	HR 4096	A2V
7	RX J1034.6+3938	10 34 38.6	+39 38 28	0.044	12.7	13.8	2001-02-17	40	HR 4067	F7V
8	RX J1117.1+6522	11 17 10.1	+65 22 07	0.147	13.0	14.0	2001-02-19	32	HR 3391	G1V
9	Ton 1388	11 19 08.7	+21 19 18	0.177	11.5	12.2	2001-02-19	16	HR 4012	F9V
10	PG 1211+143	12 14 17.7	+14 03 13	0.082	—	12.0	2001-02-19	24	HR 4864	G7V
11	Mkn 766	12 18 26.6	+29 48 46	0.013	10.6	10.6	2001-02-18	16	HR 4096	A2V
12	IC 3599	12 37 41.2	+26 42 28	0.021	13.5	13.8	2001-02-18	32	HR 4096	A2V
13	IRAS 12397+3333	12 42 10.6	+33 17 03	0.044	—	12.0	2001-02-18	24	HR 4845	G0V
14	RX J1304.2+0205	13 04 17.0	+02 05 37	0.229	—	15.6	2001-02-19	16	HR 4864	G7V
15	PG 1307+085	13 09 47.0	+08 19 48	0.155	—	13.1	2001-02-19	24	HR 4864	G7V
16	RX J1355.2+5612	13 55 16.6	+56 12 45	0.122	13.3	14.1	2001-02-19	24	HR 5280	A2V
17	PG 1402+261	14 05 16.2	+25 55 34	0.164	12.2	12.8	2001-02-18	32	HR 4845	G0V
18	Mkn 478	14 42 07.5	+35 26 23	0.077	11.1	12.2	2001-02-18	32	HR 5569	A2V
19	Mkn 493	15 59 09.7	+35 01 48	0.032	11.8	12.0	2001-02-19	16	HR 5280	A2V

Paα/Hβratio = 0.332 is expected. For only one AGN, Mkn 766 a flux ratio Brγ/Hβ can be measured. For this AGN the Brγ/Hβ flux ratio is about 3 times higher than expected for a case B (0.0275, Hummer & Storey 1987).

4. Discussion and conclusions

The main motivation for our study of NIR spectra of soft X-ray selected AGN was to search for signatures of a young starburst. The idea is that NLS1 are young AGN and therefore should show a young starburst which should be visible in the NIR spectrum. Signs of this young starburst would be the detection of strong Paα and/or Brγ emission lines in excess of what is expected from the broad Hβ and Hα line emission.

CBS 126 and RX J1355.2+5612 are the only two sources which show very high Paα/Hβ line rations. Both sources have an Hα/Hβratio = 3.5 (Grupe et al. 1999). The internal reddening of the two sources is close to the average found for the whole sample (Grupe et al. 1998b). Also the spectral analysis of the RASS data shows that the cold (neutral) absorption in soft X-rays is in agreement with no or minor intrinsic absorption. For RX J1355.2+5612 the signal-to-noise ratio at the Paα line is very low and therefore the errors in the flux measurements are large. This explains the high ratio in this source. The situation is different for CBS 126. Even though the line might be slightly affected by the correction of the atmospheric absorption troughs at around 2 μm, the line is still strong and the high flux ratio Paα/Hβ seems to be real. Displaying the Paα/Hβ ratio of CBS 126 in a Hα/Hβ vs. Paα/Hα diagram (e.g. Lacy et al. 1982; Evans & Natta 1989; Thompson 1992) shows that CBS 126 is far off most sources towards a high Paα/Hα value. The other three sources for which the Hα/Hβ ratio was available and a scaling of the spectrum by the 2MASS K magnitude was possible, RX J1007.1+2203, Ton 1388, and Mkn 478, are almost on the expected Paα/Hβ = 0.28 line in Fig. 2 in Lacy et al. (1982), which means they are not absorbed. Correcting CBS 126 for reddening reduces the Paα/Hα to 0.41, which is still a strong excess in the Paα line. A possible explanation is that this is a contribution from a nuclear starburst. In order to verify this, observations on this object with higher resolution spectroscopy have to be performed.

The clearest detection of a Brγ line was found in Mkn 766. For this source one has to take into account that it does show intrinsic optical reddening that may explain part of the high Brγ/Hβ flux ratio. The Hα/Hβ ratio is 5.9 (Grupe et al. 1998b) and its optical spectral slope $\alpha_{\rm opt}$ = 1.9, which is high compared to the rest of the sample ($< \alpha_{\rm opt} >$= 1.0; Grupe et al. 1998b). It is also a source that shows a relatively high degree of polarization of 2.3% (Goodrich 1989), while most of the sources in our sample do not show significant polarization (Grupe et al. 1998b). Arguing also for a significant absorption in Mkn 766 is the finding of Lee et al. (2001) from X-ray spectra derived from CHANDRA's LETG of a

Table 2. Results of the analysis of the NIR data. The rest-frame equivalent widths *EW* are given in Å, the *FWHM*(Paα) in $\mathrm{km\,s^{-1}}$, and the fluxes for Paα and Brγ in units of 10^{-17} $\mathrm{W\,m^{-2}}$ and 10^{-18} $\mathrm{W\,m^{-2}}$, respectively. For comparison the *FWHM*(Hβ) is listed in $\mathrm{km\,s^{-1}}$.

#	Name	Type	*EW* Pa α	*EW* Br γ	*FWHM* Paα	$F_{\mathrm{Pa}\alpha}$	$F_{\mathrm{Br}\gamma}$	$F(\mathrm{Pa}\alpha)/F(\mathrm{H}\beta)$	*FWHM*(Hβ)
1	RX J0859.0+4846	S1	160 ± 25	10 ± 5	3000 ± 100	7.5 ± 0.5[2]	3.5 ± 1.0[2]	0.40[2]	2900
2	Mkn 110	NLS1	—[3]	10 ± 5	—	—	3.7 ± 0.7[2]	—	1500
3	PG0953+414	S1	150 ± 35	—[3]	3000 ± 500	6.0 ± 0.5	—	—	3100[4]
4	RX J1005.7+4332	S1	50 ± 30	—[3]	1700 ± 1200	1.1 ± 0.4	—	0.50	2990
5	RX J1007.1+2203	NLS1	110 ± 30	25[1]	3100 ± 450	0.9 ± 0.2	0.2[1]	0.22	1400
6	CBS 126	S1	310 ± 20	5 ± 3	1600 ± 200	12.0 ± 0.5	0.3 ± 0.1	1.45	2850
7	RX J1034.6+3938	NLS1	—[3]	10[1]	—	—	0.5[1]	—	750
8	RX J1117.1+6522	NLS1	120 ± 30	—[3]	3200 ± 550	2.5 ± 0.5	—	0.60	2160
9	Ton 1388	S1	85 ± 10	—[3]	2400 ± 400	8.0 ± 1.0	—	0.20	2920
10	PG 1211+143	NLS1	200 ± 20	20[1]	1700 ± 100	12.0 ± 0.4[2]	0.3[1]	0.34[2]	1900
11	Mkn 766	NLS1	—[3]	6 ± 2	—	—	1.4 ± 0.3	—	1360
12	IC 3599	S2	—[3]	10[1]	—	—	4.0[1]	—	635
13	IRAS 12397+3333	NLS1	—[3]	10 ± 5	—	—	5.0 ± 2.0[2]	—	1900
14	RX J1304.2+0205	NLS1	—	—[3]	—	—	—	—	1400[5]
15	PG 1307+085	S1	160 ± 30	—[3]	2200 ± 100	2.7 ± 0.5[2]	—	0.15[2]	4000
16	RX J1355.2+5612	NLS1	50 ± 30	—[3]	1600 ± 1000	1.2 ± 0.6	—	3.50	1780
17	PG 1402+261	NLS1	65 ± 15	—[3]	2300 ± 250	3.7 ± 0.3	—	0.28	1700
18	Mkn 478	NLS1	50 ± 2	2[1]	1550 ± 200	8.0 ± 0.5	4.0[1]	0.27	1915
19	Mkn 493	NLS1	—[3]	10[1]	—	—	8.0[1]	—	900

[1] Upper limit.
[2] No 2MASS data available, and therefore no scaling possible to get absolute fluxes.
[3] Out of the *K*-band window.
[4] Boroson & Green (1992).
[5] *FWHM*(Hα).

dusty warm absorber in MCG–6-30-15 which has a similar X-ray spectrum as Mkn 766. However, on the other hand, Branduardi-Raymont et al. (2001) argued from their X-ray spectroscopy studies with XMM-Newtons's Reflection Grating Spectrometer (RGS, den Herder et al. 2001) that the X-ray spectral features of Mkn 766 and MCG–6-30-15 can not be explained by a dusty warm absorber alone and proposed that they are caused by gravitational redshift and relativistic broadening effects in the vicinity of a Kerr black hole.

The question remains, why the classical NLS1 in our sample, such as Mkn 478 or Mkn 493, showing strong FeII emission and weak [OIII], not show exceptionally strong NIR emission lines? The two sources that clearly have strong NIR emission line, CBS 126 and Mkn 766, are not classical NLS1. Both have strong [OIII], relatively weak FeII, and are both polarized in the optical. So far with our current data set of 19 sources, we cannot give a final answer to the question, simply for statistical reasons. Just recently, NIR spectra of two more NLS1 of our soft X-ray sample have been published, Mkn 335 and Mkn 1044 (Rodríguez-Ardila et al. 2002). Using their Paα fluxes, we derived Paα/Hβ ratios of 0.29 and 0.11, respectively. Taking the starburst galaxy sample of Coziol et al. (2001) for estimating what contribution we can expect from a usual starburst, the range of the equivalent widths *EW*(Brγ) is between 2 Å–260 Å. Based on these values we can exclude a large starburst in any of AGN in our sample. We have to extend the NIR sample in order to derive a more secure answer about which class has strong NIR emission lines. This would bring us back to our original question about the age of an AGN. Maybe the classical NLS1 are not the youngest AGN and maybe that those AGN which show also stronger [OIII] would be younger. Two facts argue for this scenario: 1) starburst galaxies always show strong [OIII]/Hβ ratio (e.g. Osterbrock 1989) and 2) recently Oshuga & Umemura (2001) suggested that Seyfert 2 galaxies are the younger AGN. In this case the strong starburst in classical NLS1 is already passed. If this is true we may ask what happens then to the only Seyfert 2 galaxy in our sample, IC 3599[1]. Shouldn't we see also strong NIR emission lines in the spectrum of this AGN? The answer is in principle yes, but the Hβ flux in this source is already rather low (see e.g. Grupe et al. 1995) and assuming a case B ratio of Hβ/Brγ = 0.0275 (Hummer & Storey 1987) we end up with the upper limit we measured in this object. In other words, IC 3599 shows a line ratio as expected, but not stronger than this either. It is interesting to note that IC 3599 has shown a strong X-ray outburst followed by a response in its optical

[1] Please note: IC 3599 can be classified as a Seyfert 1.9 galaxies based on higher resolution spectroscopy; Komossa & Bade (1999).

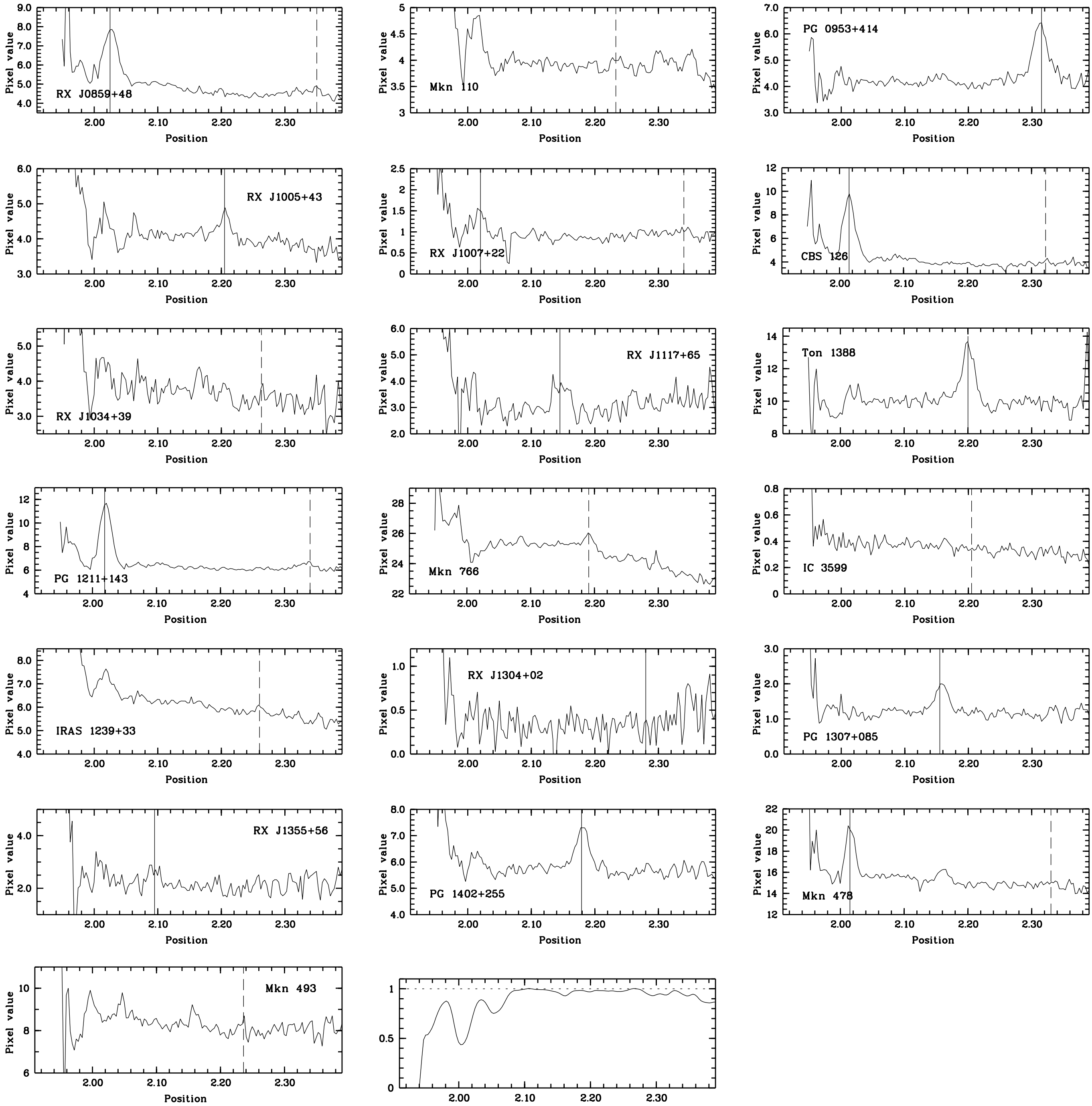

Fig. 1. NIR spectra of the 19 observed AGN; Fluxes are given in units of 10^{-15} W m^{-2} μm^{-1} and the wavelength in μm. The solid line displays the position of the Paα line and the dashed line the position of Brγ. The last spectrum shows the atmospheric transmission normalized to unity.

emission lines (Grupe et al. 1995; Brandt et al. 1995). We could have expected that when the light front passes through the center of the AGN that we would also see strong NIR lines in its spectrum. However, it seems that the light passed already the NIR emitting region. It would be interesting for future discoveries of X-ray transient AGN or galaxies to follow them also in the infrared in order to localize the NIR line emitting regions.

Our study of NIR spectra has shown that NIR spectroscopy of soft X-ray selected AGN gives interesting results. In 11 cases we were able to detect Paα emission. However, a future task should be to complete the NIR observations for the whole sample to give a more secure statement of the development of AGN. Performing the spectroscopy with higher resolution would help to search for line asymmetries as they have been reported for Hβ emission (e.g. Boroson & Green 1992). However, often strong Hβ asymmetries have been especially reported for those NLS1 with very strong FeII emission. Therefore the results of those Hβ line measurements might be influenced by the contamination of the Hβ line by FeII blends. The Paα line is not affected by FeII contamination and therefore a possible line asymmetry can be studied more accurately than in the Hβ line.

Acknowledgements. We want to thank Dr. Bev Wills for her help with the observing run and her comments on this paper. We also want to thank Dr. Dan Lester for his help and support during the CoolSpec observing run. Many thanks also to Drs. Mario Gliozzi, Stefanie Komossa, and Wolfgang Brinkmann for their comments and suggestions on the manuscript. This research has made use of the NASA/IPAC Extragalactic Database (NED) which is operated by the Jet Propulsion Laboratory, Caltech, under contract with the National Aeronautics and Space Administration and the Two Micron All Sky Survey (2MASS), which is a joint project of the University of Massachusetts and the Infrared Processing and Analysis Center/California Institute of Technology, funded by the National Aeronautics and Space Administration and the National Science Foundation. The ROSAT project is supported by the Bundesministerium für Bildung und Forschung (BMBF/DLR) and the Max-Planck-Society.

This paper can be retrieved via WWW:
`http://www.xray.mpe.mpg.de/~dgrupe/research/refereed.html`

References

Brandt, W. N., Pounds, K. A., & Fink, H. H. 1995, MNRAS, 273, L47

Branduardi-Raymont, G., Sako, M., Kahn, S. M., et al. 2001, A&A, 365, L140

Boller, Th., Brandt, W. N., & Fink, H. H. 1996, A&A, 305, 53

Boroson, T. A. 2002, ApJ 565, 78

Boroson, T. A., & Green, R. F. 1992, ApJS, 80, 109

Cid Fernandes, R., Heckman, T., Schmitt, H., González Delgado, R. M., & Storchi-Bergmann, T. 2001, ApJ, 558, 81

Coziol, R., Doyon, R., & Demers, S. 2001, MNRAS, 325, 1081

den Herder, J. W., Brinkman, A. C., Kahn, S. M., et al. 2001, A&A, 365, L7

Evans, N. J., & Natta, A. 1989, ApJ, 339, 943

Genzel, R., & Cesarsky, C. J. 2000, ARA&A, 38, 761

Gonzáles Delgado, R. M. 2001, ASP Conf. Ser., in press [astro-ph/0109505]

Goodrich, R. W. 1989, ApJ, 342, 224

Grupe, D. 1996, Ph.D. Thesis, University of Göttingen

Grupe, D., Beuermann, K., Mannheim, K., et al. 1995, A&A, 299, L5

Grupe, D., Beuermann, K., Mannheim, K., Thomas, H.-C., & Fink, H. H. 1998a, A&A, 330, 25

Grupe, D., Wills, B. J., Wills, D., & Beuermann, K. 1998b, A&A, 333, 827

Grupe, D., Beuermann, K., Mannheim, K., & Thomas, H.-C. 1999, A&A, 350, 805

Grupe, D., Thomas, H.-C., & Beuermann, K. 2001, A&A, 367, 470

Heisler, C. A., & De Robertis, M. M. 1999, AJ, 118, 2038

Hines, D. C. 1991, ApJ, 374, L9

Hoffleit, D., & Jaschek, C. 1991, The Bright star catalogue, Yale University Observatory, 5th rev. ed., ed. D. Hoffleit, & C. Jaschek

Hummer, D. G., & Storey, P. J. 1987, MNRAS, 224, 801

Ivanov, V. D., Rieke, G. H., Groppi, C. E., et al. 2000, ApJ, 545, 190

Komossa, S., & Bade, N. 1999, A&A, 343, 775

Lacy, J. H., Soifer, B. T., Neugebauer, G., et al. 1982, ApJ, 256, 75

Laor, A., Fiore, F., Elvis, M., Wilkes, B. J., & McDowell, J. C. 1997, ApJ, 477, 93

Laurent, O., Mirabel, I. F., Charmandaris, V., et al. 2000, A&A, 359, 887

Lee, J. C., Ogle, P. M., Canizares, C. R., et al. 2001, ApJ, 554, L13

Lester, D. F., Hill, G. J., Doppmann, G., & Froning, C. S. 2000, PASP, 112, 384

Mathur, S. 2000, MNRAS, 314, L17

Moran, E. C., Halpern, J. P., & Helfand, D. J. 1996, ApJS, 106, 341

Murphy, T. W., Soifer, B. T., Matthews, K., Armus, L., & Kiger, J. R. 2001, ApJ, 121, 97

Oliva, E., Origlia, L., Maiolino, R., & Moorwood, A. F. M. 1999, A&A, 350, 9

Oshuga, K., & Umemura, M. 2001, ApJ, 559, 157

Osterbrock, D. E. 1989, Astrophysics of Gaseous Nebulae and Active Galactic Nuclei (University Science Books)

Pounds, K. A., Done, C., & Osborne, J. P. 1995, MNRAS, 277, L5

Rodríguez-Ardila, A., Viegas, S. M., Pastoriza, M. G., & Prato, L. 2002, ApJ 565, 140

Terlevich, E., Diaz, A. I., & Terlevich, R. 1990, MNRAS, 242, 271

Thomas, H.-C., Beuermann, K., Reinsch, K., et al. 1998, A&A, 335, 467

Thompson, K. L. 1992, ApJ, 395, 403

Trümper, J. 1983, Adv. Space Res., 4, 241

Van der Bliek, N. S., Manfroid, J., & Bouchet, P. 1996, A&AS, 119, 547

Voges, W., Aschenbach, B., Boller, Th., et al. 1999, A&A, 349, 389

Wang, T., Brinkmann, W., & Bergeron, J. 1996, A&A, 309, 81

Wills, B. J., Laor, A., Brotherton, M. S., et al. 1999, ApJ, 515, L53